αβ T Cell Receptor-positive Cells and Interferon-γ, but not Inducible Nitric Oxide Synthase, Are Critical for Granuloma Necrosis in a Mouse Model of Mycobacteria-induced Pulmonary Immunopathology

Stefan Ehlers,[1] Jochen Benini,[1] Heinz-Dieter Held,[2]
Christiane Roeck,[1] Gottfried Alber,[3] and Stefan Uhlig[2]

[1]*Divisions of Molecular Infection Biology and* [2]*Pulmonary Pharmacology, Research Center Borstel, Center for Medicine and Biosciences, D-23845 Borstel, Germany*
[3]*Institute of Immunology, College of Veterinary Medicine, D-04103 Leipzig, Germany*

Abstract

The immunological basis of tuberculin-induced necrosis, known for more than a century as "Koch's phenomenon," remains poorly understood. Aerosol infection in mice with the highly virulent *Mycobacterium avium* strain TMC724 causes progressive pulmonary pathology strongly resembling caseating necrosis in human patients with tuberculosis. To identify the cellular and molecular mediators causing this pathology, we infected C57BL/6 mice and mice selectively deficient in recombinase activating gene (RAG)-1, αβ T cell receptor (TCR), γδ TCR, CD4, CD8, β2-microglobulin, interferon (IFN)-γ, interleukin (IL)-10, IL-12p35, IL-12p35/p40, or iNOS with *M. avium* by aerosol and compared bacterial multiplication, histopathology, and respiratory physiology in these mice. The bacterial load in the lung was similarly high in all mouse groups. Pulmonary compliance, as a surrogate marker for granulomatous infiltrations in the lung, deteriorated to a similar extent in all groups of mice, except in αβ TCR-knockout (KO) and IL-12–KO mice in which compliance was higher, and in IFN-γ and inducible nitric oxide synthase–KO mice in which compliance was reduced faster. Progressive caseation of pulmonary granulomas never occurred in αβ TCR-KO, IL-12–KO, and IFN-γ–KO mice and was reduced in CD4-KO mice. In summary, αβ TCR^+ cells and IFN-γ are essential for the development of mycobacteria-induced pulmonary caseous necrosis. In contrast, high mycobacterial load and extensive granulomatous infiltration per se are not sufficient to cause caseation, nor is granuloma necrosis linked to the induction of nitric oxide.

Key words: tuberculosis • granuloma • necrosis • Koch's phenomenon • immunopathology

Introduction

Granuloma formation is a hallmark of mycobacterial infections and represents the histological correlate of both protective immunity and inflammatory tissue destruction (1–3). In human tuberculosis (TB)*, granuloma macrophages activated by T cells can effectively restrain the growth of mycobacteria but may also undergo necrosis in central areas of the granulomas (4, 5). This "caseous" center may subsequently liquefy and erode into a bronchus spreading *Mycobacterium tuberculosis* into the environment (6). Therefore, granuloma necrosis and cavity formation do not only contribute to the pathology in an infected individual, but are also significantly involved in the spreading of the disease. In addition, because antimycobacterial drugs may not sufficiently penetrate into caseous lesions, curative chemotherapy may be compromised (7). Since TB currently affects 10 million new patients each year and kills ~3 million of them world-wide (8, 9), elucidation of the mechanisms that cause this epidemiologically relevant pathology could lead to new preventive or therapeutic strategies.

While the mediators of cellular recruitment into the granuloma and the structural organization of the granuloma itself have been studied in some detail (10), no experimental data are available concerning the cellular and mo-

Address correspondence to Stefan Ehlers, Division of Molecular Infection Biology/Research Center Borstel, Center for Medicine and Biosciences, Parkallee 22, D-23845 Borstel, Germany. Phone: 49-4537-188481; Fax: 49-4537-188686; E-mail: sehlers@fz-borstel.de

**Abbreviations used in this paper:* β2M, β2-microglobulin; DTH, delayed-type hypersensitivity; iNOS, inducible nitric oxide synthase; KO, knockout gene-deficient; RAG, recombinase activating gene; TB, tuberculosis.

lecular mechanisms that mediate granuloma necrosis. This is due to the fact that the most commonly used animal model, the laboratory mouse, does not show granuloma necrosis in response to aerosol infection with *M. tuberculosis*, but characteristically develops a chronic fibrosis of the infected lung (11, 12). On the other hand, guinea pigs and rabbits do develop caseating necrosis as a consequence of *M. tuberculosis* infection (13–15), but most immunological reagents, including gene-deficient strains, are not available for these species.

We described previously an infection model in immunocompetent mice whose pulmonary pathology strongly resembles that characteristic of TB patients (16). A highly virulent strain of *M. avium*, TMC724, when inhaled by mice induces a progressive granulomatous response which, after the 14th wk of infection, invariably necrotizes at the center. Importantly, this type of necrosis differs from that apparent in immunodeficient mice infected with *M. tuberculosis*, where widespread parenchymal tissue necrosis develops (10, 17), in that a well-defined border of epithelioid macrophages surrounded by perigranulomatous fibrosis seals off the caseating center of the granuloma (16).

Here, we made use of this mouse model of mycobacteria-induced pulmonary granuloma necrosis in order to investigate whether lymphocytes, and if so, which subset of lymphocytes would be necessary to initiate this degenerative event. Furthermore, we investigated the role of the principal macrophage activating cytokine, IFN-γ, and of the cytokines regulating its expression, IL-10 and IL-12, in causing granuloma necrosis, by using mouse strains selectively deficient for these mediators. Since both the bacterial load and the overall amount of inflammatory infiltration could also be key factors, we simultaneously monitored bacterial growth and pulmonary physiology in infected mice over time. Our data support the view that the presence of αβ TCR-bearing cells and the presence of IFN-γ are essential for granuloma necrosis in this murine model of mycobacteria-induced immunopathology. Although the precise molecular mechanisms by which IFN-γ triggers granuloma necrosis remain to be elucidated, our study rules out a critical role for inducible nitric oxide.

Materials and Methods

Mice. C57BL/6 were purchased from Charles River Laboratories. The following selectively gene-deficient (knockout [KO]*) mice were purchased from The Jackson Laboratory: recombinase activating gene (RAG)-1–KO, αβ TCR-KO, γδ TCR-KO, CD4-KO, CD8-KO, β2-microglobulin (β2M)-KO, IFN-γ–KO, and NOS2-KO (all at least 5th generation backcrosses to a C57BL/6 background). Mice deficient in IL-12p35, IL-12p35/p40, or MHC class II (all at least 5th generation backcrosses to a C57BL/6 background) were provided by H. Mossmann, Max-Planck-Institute for Immunobiology, Freiburg, Germany. IL-10-KO mice were 10th generation backcrosses to a C57BL/10 background, and C57BL/10 mice were used as controls in experiments involving IL-10–KO mice. All mice were free of 17 viral mouse pathogens and common bacterial or parasitic diseases. For the course of *M. avium* infection, age- and sex-matched groups of mice were housed in isolator cages under barrier conditions in the animal facilities at the Borstel Research Center. All mouse experiments were approved by the Schleswig-Holstein Ministry of the Environment, Nature and Forestation, and an independent Institutional Review Board.

Bacteria. *M. avium* TMC724 (originally obtained from the Trudeau Institute) was passaged in C57BL/6 mice and cultured in Middlebrook 7H9 (Difco) medium supplemented with oleic acid, albumin, dextrose, and catalase (Becton Dickinson) to a late logarithmic phase. Aliquots were frozen at −70°C until needed. An inoculum of bacteria was prepared by thawing several aliquots, washing them by centrifugation at 16,000 *g* for 15 min, and pooling the pellets in distilled water. Aerogenic infection was performed in a Glas-Col aerosol infection device (Glas-Col). Mice were exposed for 40 min to an aerosol generated by nebulizing ~5.5 ml of a suspension containing 10^9 CFU/ml *M. avium* TMC724. Inoculum size (~10^5 CFU/lung) was checked 24 h after infection by determining the bacterial load in the lungs of infected mice. Mice were scored as moribund and killed when weight loss was in excess of 30% compared with age-matched uninfected controls. Groups of 4–6 mice were anaesthetized and killed at indicated time points to follow the course of infection. Lungs were removed aseptically and homogenized in 3 ml of distilled water to determine bacterial loads by plating serial 10-fold dilutions of whole lung homogenates on nutrient Middlebrook 7H10 agar (Difco) supplemented with oleic acid albumin, dextrose, and catalase. Bacterial colony numbers (CFUS) were determined after 21-d incubation at 37°C in humidified air. Data for different KO mouse strains were obtained in separate experiments, each having its own control group, and are therefore presented in individual graphs. The natural course of infection and the kinetics of granuloma formation in C57BL/6 mice infected with *M. avium* TMC724 were described previously (16). There was no difference in the kinetics of granuloma necrosis in C57BL/6 and C57BL/10 mice.

Histology. A 22-gauge catheter was inserted via a small incision into the trachea of anaesthetized mice and the lungs were filled with fixative solution (4% formalin in PBS, pH 7.4) under a hydrostatic pressure of 20–25 cm fluid column. Fixation was left to proceed until all lung lobes were well expanded. The trachea was clamped and the lung was removed in total and submerged in fresh 4% formalin solution for ~3 d, after which lungs were embedded in paraffin. 3–5-μm sections were cut on a rotary microtome (RM 2155; Leica), stretched in a water bath, and mounted on glass slides. Sections were left to dry for 2 h at 37°C. Slides were stained with standard Hematoxylin stains. Although most experiments involving KO mouse strains were performed independently, each with its own set of infected control C57BL/6 mice, Fig. 2 only shows one representative micrograph for C57BL/6 mice at 19 wk after infection, because lungs of infected C57BL/6 and C57BL/10 mice always gave the same results.

Isolated Ventilated and Perfused Mouse Lung. The mouse lungs were prepared and perfused at indicated time points after infection essentially as described recently (18, 19). Briefly, lungs were perfused in a nonrecirculating fashion through the pulmonary artery at a constant flow of 1 ml/min resulting in a pulmonary artery pressure of 2–3 cm H_2O. As a perfusion medium we used RPMI 1640 medium lacking phenol red (Biowhittaker) at 37°C and containing 4% low endotoxin grade albumin (Serva). The lungs were ventilated by negative pressure (−2 cm H_2O to −10 cm H_2O) at a rate of 90 breaths/min. Artificial thorax chamber pressure was measured with a differential pressure transducer (DP 45–24; Validyne), and the airflow rate was measured with a

Fleisch-type pneumotachograph tube connected to a differential pressure transducer (DP 45–15; Validyne). Arterial pressure was continuously monitored by means of a pressure transducer (Isotec Healthdyne) that was connected to the cannula ending in the pulmonary artery. All data were transmitted to a computer and analyzed with Pulmodyn software (Hugo Sachs Elektronik). Tidal volume (V_T) was derived by integration of the flow rate, and the data were analyzed by applying the formula: $P = 1/C \cdot V_T + R_L \cdot dV_T/dt$, where P is chamber pressure, C is pulmonary compliance, and R_L lung resistance. All compliance data shown were obtained after 20 min of perfusion and ventilation.

Statistics. Quantifiable data (CFU counts, pulmonary compliance) were analyzed using Student's *t* test. For multiple comparisons, one-way ANOVA and Tukey's posttest were used. Means, SDs, confidence intervals, and statistics were calculated using GraphPad Prism version 3.00 for Windows (GraphPad Software, San Diego, CA; www.graphpad.com).

Results

Histopathology, Bacterial Load, and Pulmonary Compliance in C57BL/6 Mice Aerogenically Infected With M. avium. After aerosol infection with 10^5 CFU *M. avium* TMC724, there was progressive growth of the organism until a plateau was reached at $\sim 10^{10}$ CFU per lung (Fig. 1 A). Starting around week 14 after infection, mice exhibited signs of dyspnea and hyperventilation, and appeared moribund by ~20 wk after infection.

Using isolated and perfused mouse lungs of infected animals we measured pulmonary compliance to establish an independent parameter reflecting alveolar and interstitial space occupied by inflammatory infiltrations. Data obtained at various time points in a typical experiment are shown in Fig. 1 B. Pulmonary compliance deteriorated progressively in infected mice, dropping below 10 μl/cm H_2O at around 14 wk after infection and falling as low as 5 μl/cm H_2O when mice became moribund. In contrast, uninfected control mice showed a slight increase in their pulmonary compliance as they grew older, which was generally in the same range as reported before (18). Fig. 1 C summarizes data from a total of six experiments showing all individual measurements and the 95% confidence interval of data points taken during two late time points of infection. Although there was some variability in individual mice, it is evident that respiratory insufficiency was the likely cause of death in infected mice.

After aerosol infection, a distinct pattern of progressive pulmonary pathology developed, as described previously (16). At ~10 wk after infection, there was widespread infiltration of alveolar and interstitial space with epithelioid and foamy macrophages, occupying up to one-half of the lung. Most of these macrophages showed signs of being activated because they stained positive for inducible nitric oxide synthase (iNOS; data not shown). Lymphocytes were apparent in aggregated form, located for the most part on the periphery of these massive infiltrations. At ~14 wk after infection, granulomatous infiltrations further coalesced, and first signs of irreversible cell damage appeared, such as condensation of nuclei and small foci of nuclear debris within

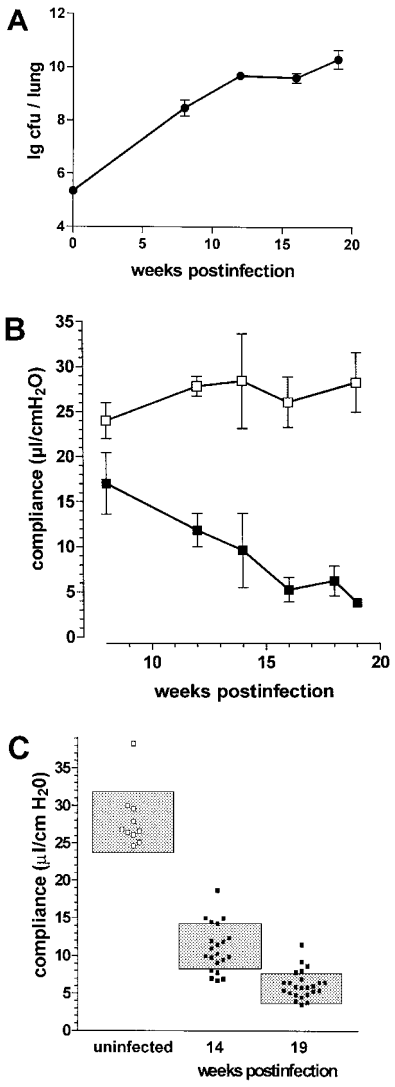

Figure 1. Course of aerosol infection with *M. avium* in immunocompetent mice C57BL/6 mice were infected with $\sim 10^5$ CFU *M. avium* TMC724 by aerosol. (A) Bacterial growth was followed in lungs over time (mean CFU of six mice per group ± SD). (B) Pulmonary compliance was measured in uninfected (white squares) and infected mice (black squares) over time (means of three mice per group ± SD). C shows a compilation of individual compliance measurements from a total of six experiments (white squares, uninfected mice at 14 and 19 wk after infection; black squares, aerosol-infected mice at 14 and 19 wk after infection). The shaded areas represent the 95% confidence interval of all data collected at the indicated time point.

macrophage-rich areas. Finally, 2–3 wk before animals were killed due to their deteriorating general condition, full-blown caseating necrosis was evident in the majority of granulomatous lesions of the lung of all mice (Fig. 2 A and B). Caseous necrosis uniformly occurred at the center of the granulomas which had been occupied previously by heavily infected macrophages (15). Caseous centers were surrounded by a variably thick zone of degenerating neutrophils, which in turn was demarcated from the remaining lung tissue by a wide layer of macrophages that appeared, by light-microcospic criteria, as epithelioid (insert in Fig. 2

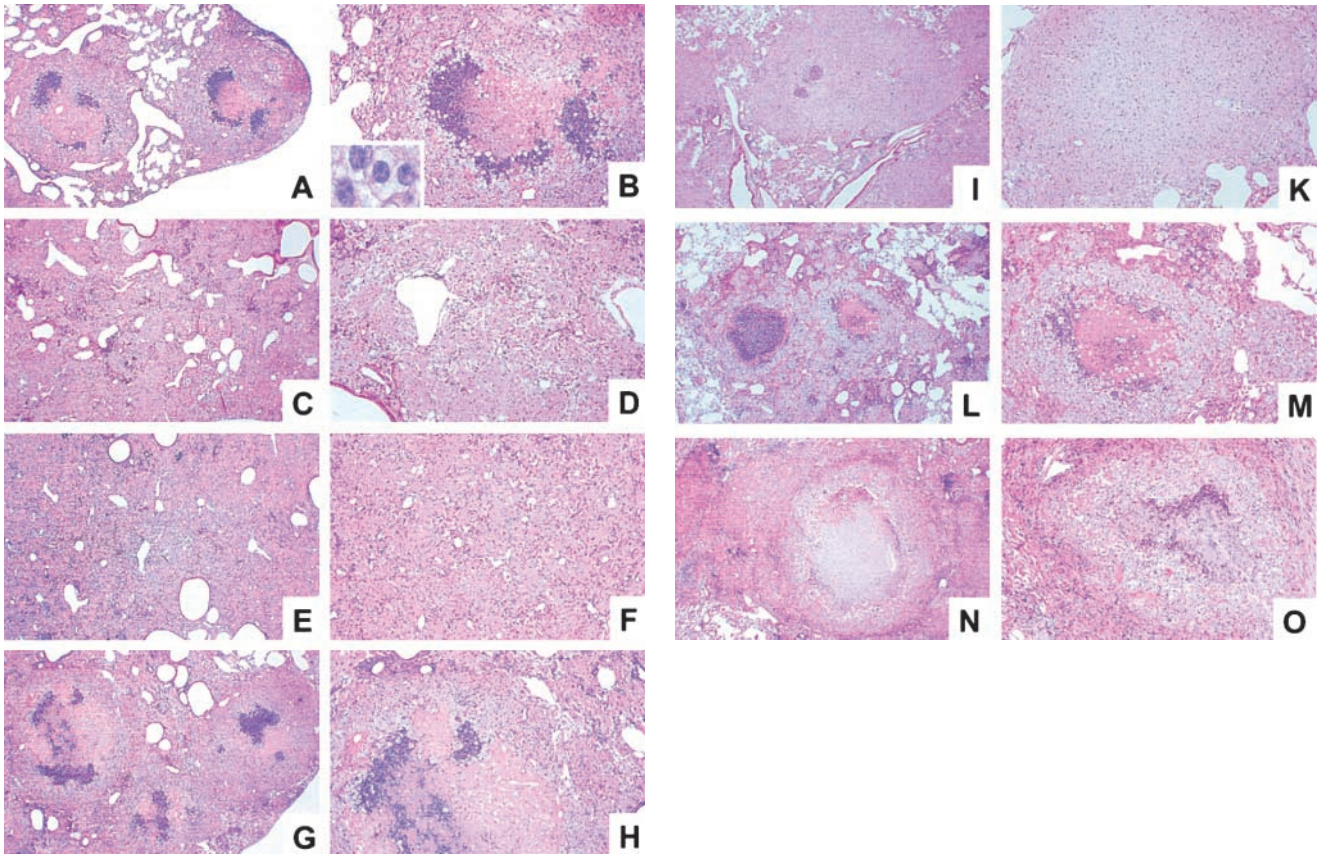

Figure 2. Histopathology of lungs from immunocompetent and T cell subset–deficient mice at 19 wk infection with *M. avium*. Mice were infected with ~10^5 CFU *M. avium* TMC724 by aerosol, and lungs from infected mice were removed at 19 wk after infection and processed for H&E staining. Low-power micrographs shown are representative of at least three mice per group (A, C, E, G, I, L, and N, original magnifications: ×12; B, D, F, H, K, M, and O, original magnifications: ×32; insert in B, original magnification: ×320). (A and B) C57BL/6 mice. (C and D) RAG-1–KO. (E and F) αβ TCR-KO mice. (G and H) γδ TCR-KO mice. (I and K) CD4-KO mice. (L and M) CD8-KO mice. (N and O) β2M-KO mice.

B). For the comparison of histological sections described below, we chose the time point at 19 wk after infection.

Since progressive lesion development strongly correlated with progressively deteriorating compliance in infected mice, it appeared feasible to use impairment of respiratory function measured by compliance as a quantitative surrogate parameter for increasing infiltration of total lung space.

Granulomatous Lesions in C57BL/6 and RAG-1–KO, αβ TCR-KO, γδTCR-KO, CD4-KO, CD8-KO, β2M-KO, and MHC Class II-KO Mice Aerogenically Infected with M. avium. First, we wished to establish whether specific lymphocytes were involved in granuloma necrosis after *M. avium* infection. When RAG-1–KO mice deficient in B and T lymphocytes were infected, caseation did not occur at any time point examined. In moribund mice at 19 wk after infection there were a few necrotic cells, isolated or in groups, scattered throughout the extensive sheets of foamy and epithelioid macrophages, but the characteristic feature of large, well-demarcated centrally caseating lesions present in immunocompetent mice was never apparent (Fig. 2 A and B versus C and D). Thus, caseous granuloma necrosis depends on the presence of specific lymphocytes.

Next, we wished to determine whether T cells and which T cell subset might be responsible for the induction of granuloma necrosis. When mice deficient for either the αβ TCR or the γδ TCR were infected, it became evident that only mice bearing the αβ TCR were capable of developing caseous necrosis (Fig. 2 A and B). At 19 wk after infection, αβ TCR-KO mice had a few necrotic cells scattered over the entire lung, but never showed the pathognomonic structure of centrally caseating granulomas (Fig. 2 E and F). In contrast, γδ TCR-KO mice were no different from immunocompetent mice regarding the extent and morphological aspect of granuloma necrosis (Fig. 2 G and H).

Next, we examined pulmonary pathology in mice deficient for individual T cell subsets. Most CD4-deficient mice exhibited only few "pockets" of dead or dying cells dispersed throughout the granulomatous infiltrations (Fig. 2 K). Some moribund mice deficient for CD4 also showed incipient necrotic foci at the centers of epithelioid macrophage agglomerations, but these were never as prominent in size and as typically organized as in C57BL/6 mice (Fig. 2 I). When the experiment was repeated, an additional

group of MHC class II–deficient mice was also examined. These mice showed no signs at all of necrosis within the extensive sheets of epitheliod macrophages infiltrating the lung at 19 wk after infection (data not shown). CD8-deficient and β2M-KO mice developed granuloma necrosis to the same extent and with a similar appearance as infected wild-type mice (Fig. 2 L–O). In summary, the major contributor to central granuloma necrosis within the αβ TCR-bearing subset is in the MHC class II–restricted $CD4^+$ T cell compartment.

Bacterial Load and Compliance in the Lungs of C57BL/6 and RAG-1–KO, αβ TCR-KO, γδ TCR-KO, CD4-KO, and CD8-KO Mice Aerogenically Infected with M. avium. The failure to develop central caseation in RAG-1–KO, αβ TCR-KO and, to a large extent, in CD4-KO mice, could be a result of different bacterial loads in the lungs of these mice, or of altered kinetics or extent of inflammatory cell infiltration. However, there was no difference between RAG-1–KO and C57BL/6 mice in terms of CFU counts in either lung (Fig. 3 A), liver or spleen (data not shown) at both 14 and 19 wk after infection. αβ TCR-KO mice did have higher CFU counts in their lungs at 14 wk after infection, but this was no longer statistically significant at 19 wk after infection when histopathology was compared (Fig. 3 B). CD4-KO, CD8-KO, and β2M-KO mice showed the same bacterial load as control C57BL/6 mice when examined at either 14 or 19 wk after infection (Fig. 3 C). Therefore, high mycobacterial load per se is not correlated with onset of granuloma necrosis.

Concerning overall diminution of pulmonary elasticity due to inflammatory cell influx, there was a tendency in RAG-1–KO mice to have a slightly better pulmonary compliance at 14 wk after infection, but this was not statistically significant (Fig. 4 A). Likewise, αβ TCR-KO mice had a less severe reduction in pulmonary compliance, start-

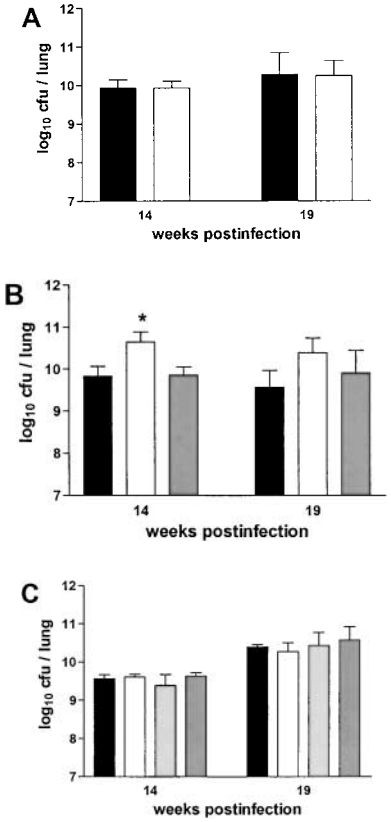

Figure 3. Bacterial loads in immunocompetent and T cell subset–deficient mice after aerosol infection with *M. avium*. Mice were infected with ~10^5 CFU *M. avium* TMC724 by aerosol, and bacterial growth was determined in the lungs at indicated time points after infection. Data are the mean CFU ± SD of 4–6 mice per time point. (A) C57BL/6 mice (black bars), RAG-1–KO mice (white bars). (B) C57BL/6 mice (black bars), αβ TCR-KO mice (white bars), γδTCR-KO mice (gray bars). (C) C57BL/6 mice (black bars), CD4-KO mice (white bars), CD8-KO mice (light gray bars), β2M-KO mice (dark gray bars). $^*P < 0.05$ vs. C57BL/6.

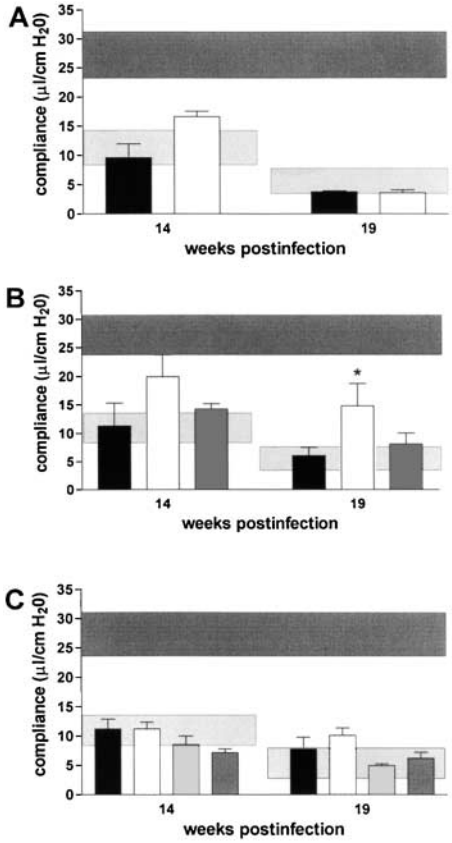

Figure 4. Pulmonary compliance in immunocompetent and T cell subset–deficient mice after aerosol infection with *M. avium*. Mice were infected with ~10^5 CFU *M. avium* TMC724 by aerosol, and pulmonary compliance was determined in the isolated and perfused mouse lungs at indicated time points after infection. For purposes of interassay data comparability, the horizontal areas shaded in dark gray represent the 95% confidence interval of measurements from six independent experiments in uninfected mice (Fig. 1 C), and the horizontal areas shaded in light gray represent the 95% confidence interval of measurements taken in infected C57BL/6 mice from six independent experiments (Fig. 1 C). (A) C57BL/6 mice (black bars), RAG-1–KO mice (white bars). (B) C57BL/6 mice (black bars), αβ TCR-KO mice (white bars), γδ TCR-KO mice (gray bars). (C) C57BL/6 mice (black bars), CD4-KO mice (white bars), CD8-KO mice (light gray bars), β2M-KO mice (dark gray bars). Data are the means ± SD of 3–6 mice per group. $^*P < 0.05$ vs. C57BL/6 and γδ TCR-KO mice.

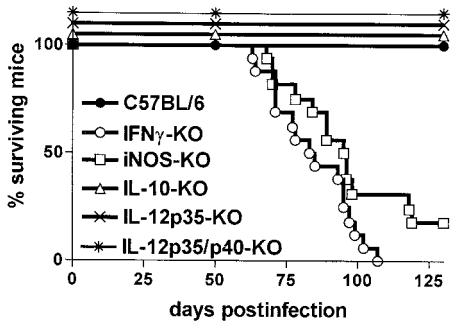

Figure 5. Survival of various cytokine- or iNOS-deficient mouse strains after aerosol infection with *M. avium*. Mice were infected with ~10^5 CFU *M. avium* TMC724 by aerosol, and moribund mice were killed. Data shown are the percentage of surviving mice, the total number of mice per group ranging from 12 to 16.

ing at 14 wk after infection, and reaching statistical significance at 19 wk after infection (Fig. 4 B). CD4-KO, CD8-KO, and β2M-KO mice had similar loss of pulmonary elasticity at 14 and 19 wk after infection as infected C57BL/6 mice (Fig. 4 C). At 19 wk after infection, when granuloma necrosis was compared histologically, there was no difference in pulmonary compliance between any of the different KO-mouse strains (with the exception of αβ TCR-KO mice) and simultaneously infected C57BL/6 mice (Fig. 4 A–C). In summary, the development of caseous necrosis in immunocompetent mice as opposed to RAG-1–KO or CD4-KO mice is not related to differentially altered pulmonary compliance in these mice.

Granulomatous Lesions in C57BL/6 and IFN-γ–KO, IL-10–KO, IL-12p35-KO, IL-12p35/p40-KO, and iNOS-KO Mice Aerogenically Infected with M. avium. Determination of cytokine mRNA levels in lung homogenates from C57BL/6, RAG-1–KO, and αβ TCR-KO mice aerogenically infected with *M. avium* revealed that KO mice consistently had ~10-fold lower levels of IFN-γ mRNA in lesion-harboring lungs than wild-type mice (data not shown). Therefore, we wished to establish whether IFN-γ was causally involved in granuloma necrosis. In a typical aerosol infection with *M. avium*, IFN-γ–KO mice started to become moribund as early as day 70 after infection, and all IFN-γ–KO mice were dead by 15 wk after infection (Fig. 5). When histopathology was examined, there was advanced leukocyte infiltration already at 10 and 14 wk after infection. Infiltrations in IFN-γ–KO mice appeared highly disorganized and of mixed cellularity with a high proportion of neutrophils (insert in Fig. 6 D). Despite this excessive cellular influx, caseation did not occur at any time point examined in IFN-γ–KO mice. When the experiment was repeated, three IFN-γ–KO mice survived until week 19 after infection, but again showed no signs of caseating necrosis despite massive pulmonary granulocyte infiltration (Fig. 6 C and D).

Since the expression of IFN-γ is regulated by both IL-12 and IL-10, we next determined whether the absence of

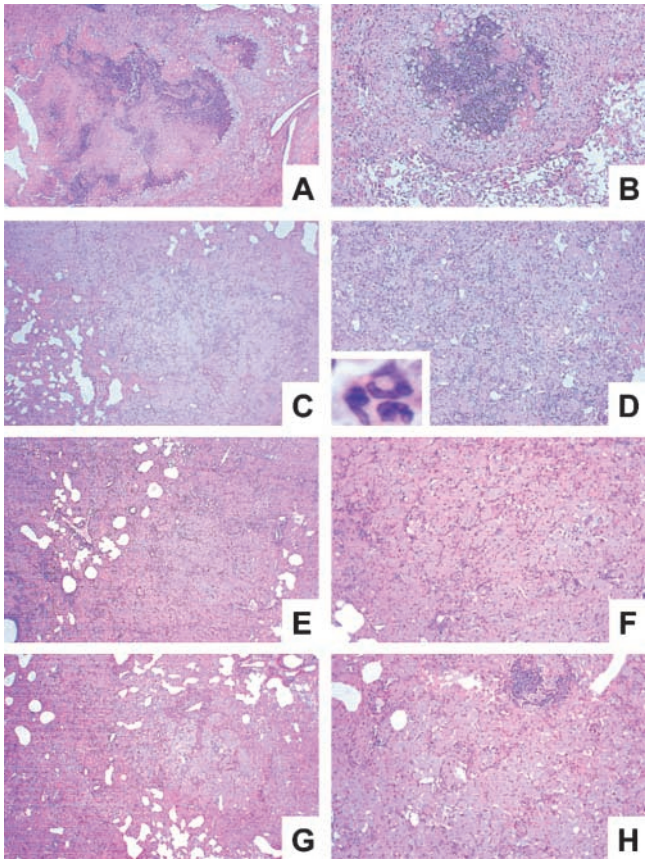

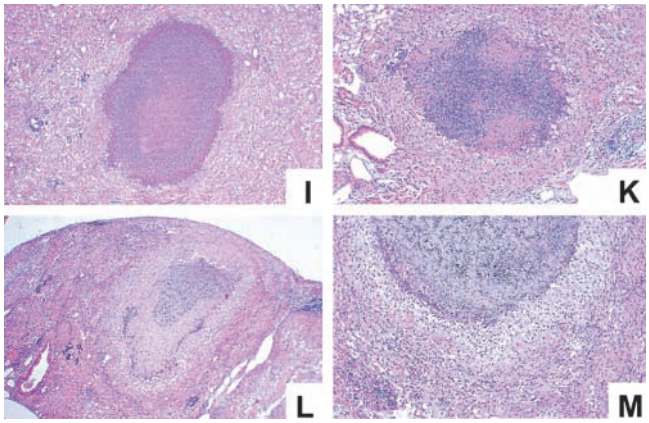

Figure 6. Histopathology of lungs from immunocompetent and cytokine- or iNOS-deficient mice at 19 wk after infection with *M. avium*. Mice were infected with ~10^5 CFU *M. avium* TMC724 by aerosol, and lungs from infected mice were removed at 19 wk after infection and processed for H&E staining. Micrographs shown are representative of at least three mice per group (A, C, E, G, I, and L, original magnifications: ×12; B, D, F, H, K, and M, original magnifications: ×32; insert in D, original magnification: ×20). (A and B) C57BL/6 mice. (C and D) IFN-γ–KO mice. (E and F) IL-12p35-KO mice. (G and H) IL-12p35/p40-KO mice. (I and K) IL-10–KO mice. (L and M) iNOS-KO mice.

these cytokines would also impact on granuloma necrosis after aerosol *M. avium* infection. Gene-targeted mouse strains, lacking either only p35 or both the p35 and the p40 component of IL-12, survived the entire 20-wk examination period (Fig. 5). In both strains, there was extensive granulomatous infiltration composed almost exclusively of epithelioid cells, but caseous necrosis was conspicuously absent (Fig. 6 E–H). In contrast, IL-10–KO mice showed advanced signs of granuloma necrosis as early as 14 wk after infection and exhibited marked central caseation of granulomatous lesions at 19 wk after infection, similar to infected wild-type controls (Fig. 6 I and K).

Since nitric oxide is a known effector of both inflammatory and antibacterial responses induced by IFN-γ, mice deficient for iNOS-KO were also infected with *M. avium* via aerosol. Infected iNOS-KO mice became moribund in a similar time frame as infected IFN-γ–KO mice (Fig. 5). Although granuloma necrosis appeared to occur less frequently and in a somewhat delayed fashion, it was clear that massive central necrotization of epithelioid granulomas was present in surviving mice at 19 wk after infection (Fig. 6 L and M).

In summary, IFN-γ is necessary for granuloma necrosis in this murine model of mycobacteria-induced immunopathology, but the mechanism of necrotization is independent of iNOS.

Bacterial Load and Compliance in the Lungs of C57BL/6 and IFN-γ–KO, IL-10–KO, IL-12p35-KO, IL-12p35/p40-KO, and iNOS-KO Mice Aerogenically Infected with M. avium. The failure to develop central caseation in IFN-γ–KO and IL-12–KO mice could be a result of different bacterial loads in the lungs of these mice, or of altered kinetics or extent of inflammatory cell infiltration. However, there was no significant difference between IL-12p35-KO, IL-12p35/p40-KO, and C57BL/6 mice in terms of CFU counts in either lung (Fig. 7 B), liver, or spleen (data not shown) at both 14 and 19 wk after infection. IL-10–KO mice also had comparable bacterial loads in these organs (Fig. 7 C). IFN-γ-KO mice had significantly higher CFU counts in their lungs at 10 wk (data not shown) and 14 wk after infection. (Fig. 7 A). In contrast, iNOS-KO mice had significantly lower bacterial counts in their lungs at 14 and 19 wk after infection. (Fig. 7 D), corroborating the interpretation that high mycobacterial load per se is not correlated with onset of granuloma necrosis.

Although there was a tendency for IL-12p35/p40-KO mice to have a better compliance than IL-12p40 producing IL-12p35-K0 mice at 14 wk after infection, this was not statistically significant. Both IL-12–deficient strains, lacking either only p35 or both p35/p40 chains of IL-12, had a profoundly better pulmonary compliance at 19 wk after infection than infected wild-type mice (Fig. 8 B). IL-10–KO mice had a similar loss of pulmonary elasticity at 14 and 19 wk after infection as infected syngenic wild-type mice (Fig. 8 C). In contrast, both IFN-γ-KO and iNOS-KO mice had dramatically reduced pulmonary elasticity already at 14 wk after infection, and respiratory insufficiency became incompatible with life before 19 wk after infection in most of these mice (Fig. 8 A and D). In summary, the absence of caseous necrosis in IL-12-KO or IFN-γ–KO mice (as opposed to immunocompetent mice) is not directly correlated with altered pulmonary compliance in these immunodeficient mice, whereas early death of IFN-γ–KO and iNOS-KO mice can be explained by advanced pulmonary insufficiency.

Discussion

Robert Koch was the first to describe the phenomenon in guinea pigs that ~6 wk after establishment of infection

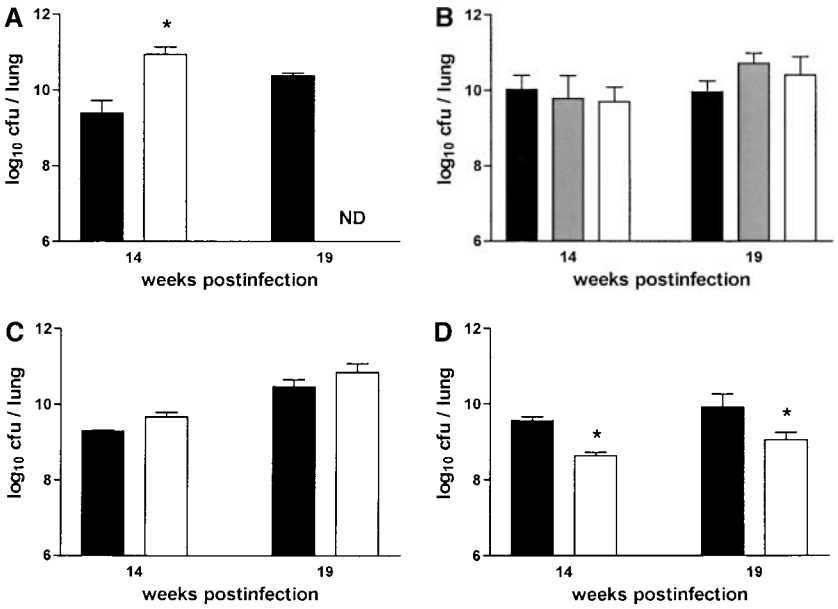

Figure 7. Bacterial loads in immunocompetent and cytokine- or iNOS-deficient mice after aerosol infection with *M. avium*. Mice were infected with ~10^5 CFU *M. avium* TMC724 by aerosol, and bacterial growth was determined in the lungs at indicated time points after infection. Data are the mean CFU ± SD of 4–6 mice per time point. (A) C57BL/6 mice (black bars), IFN-γ–KO mice (white bars), ND, not determined due to premature death of mice. (B) C57BL/6 mice (black bars), IL-12p35-KO mice (gray bars), IL-12p35/p40-KO mice (white bars). (C) C57BL/10 mice (black bars), IL-10–KO mice (white bars). (D) C57BL/6 mice (black bars), iNOS-KO mice (white bars). $^*P <$ 0.05 vs. C57BL/6.

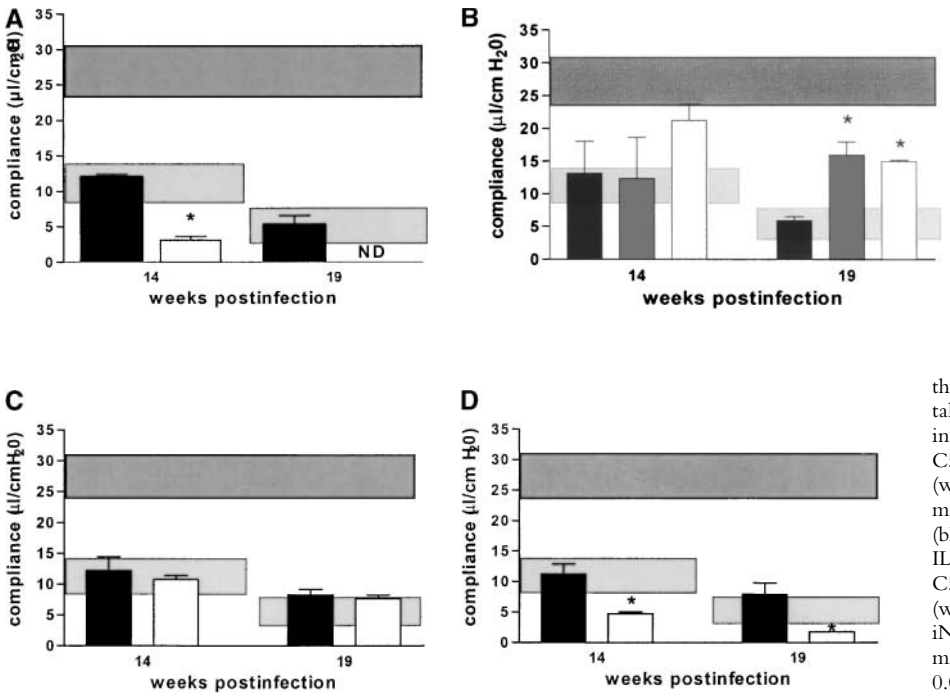

Figure 8. Pulmonary compliance in immunocompetent and cytokine- or iNOS-deficient mice after aerosol infection with *M. avium*. Mice were infected with ~10^5 CFU *M. avium* TMC724 by aerosol, and pulmonary compliance was determined in the isolated and perfused mouse lungs at indicated time points after infection. For purposes of inter-assay data comparability, the horizontal areas shaded in dark gray represent the 95% confidence interval of measurements from six independent experiments in uninfected mice (Fig. 1 C), and the horizontal areas shaded in light gray represent the 95% confidence interval of measurements taken in infected C57BL/6 mice from six independent experiments (Fig. 1 C). (A) C57BL/6 mice (black bars), IFN-γ–KO mice (white bars), ND, not determined due to premature death of mice. (B) C57BL/6 mice (black bars), IL-12p35-KO mice (gray bars), IL-12p35/p40-KO mice (white bars). (C) C57BL/10 mice (black bars), IL-10–KO mice (white bars). (D) C57BL/6 mice (black bars), iNOS-KO mice (white bars). Data are the means ± SD of three mice per group. $^*P <$ 0.05 vs. C57BL/6 mice.

with *M. tuberculosis*, intradermal challenge with whole organisms results in necrosis both at the site of injection and in the original tuberculous lesion (20, 21). These potentially harmful effects of specific delayed-type hypersensitivity (DTH) and, more particularly, their relationship to cell-mediated protective immunity capable of containing growth of *M. tuberculosis* have been the subject of considerable debate and confusion (1, 6, 22, 23). In essence, however, the cellular and molecular mediators responsible for this type of necrosis have thus far defied experimental definition. This is largely due to the lack of an animal model which would adequately reflect the mycobacteria-induced immunopathology present in human TB patients, i.e., caseating granuloma necrosis, and, at the same time, permit selective manipulation of isolated components of the immune system.

Using selectively gene-deficient mice in a model system which strongly resembles human pathology, we now unequivocally show that αβ TCR-bearing cells, but not γδ TCR-bearing cells, are necessary for granuloma necrosis, and that this degenerative event is predominantly accounted for by the MHC class II–restricted $CD4^+$, but not the $CD8^+$ T cell subset. In addition, we show that IFN-γ is necessary for granuloma necrosis to occur, but that IFN-γ does not mediate necrotization by inducing nitric oxide. We further provide evidence that neither bacterial load, nor the overall amount of inflammatory infiltration per se are ultimately decisive for granuloma caseation. On the other hand, the death of infected mice, particularly the premature death in mice with a deficiency for IFN-γ or iNOS, does not correlate with the onset of granuloma necrosis, but is more closely associated with the extent of respiratory distress due to excessive inflammatory infiltrates in these mice.

Some unique features of the model system used contributed to the findings detailed in this report. The first concerns the choice of organism used for infection. *M. avium* is an opportunistic pathogen in humans mostly affecting patients with a local or systemic immunodeficiency (24). In immunocompetent children and adults, however, it sometimes leads to a clinico-pathological presentation not dissimilar to TB (25). In mice, the causative organism of TB, *M. tuberculosis*, causes chronic fibrosis (11, 26), whereas, fortuitously, *M. avium* infection induces a pathology highly similar to that found in human TB (16, 27). It is obvious that protection and immunity can best be studied in model systems using the causative organism itself (28, 29). However, the mechanisms involved in the immunopathology of TB may only be accessible, at least in the mouse, in an infection model mimicking the pathology of human TB.

Because TMC724 is so virulent already in immunocompetent mice and because select immunodeficiencies hardly affect its growth rate in vivo, another common confounding factor when examining the course of infection in KO mouse models, i.e., differential bacterial growth, is of little relevance in this model. This latter feature has enabled us to determine that high bacterial load is not sufficient to induce granuloma necrosis, since IFN-γ–KO and αβ TCR-KO mice had the highest bacterial counts in their organs, yet showed no signs of centrally necrotizing granulomas. On the other hand, *M. avium*-infected iNOS-KO mice exhibited significantly lower CFU counts in the lungs, as was reported previously for the liver and spleen after intravenous infection with this *M. avium* strain in these mice (30). However, iNOS-KO mice aerogenically infected with *M. avium* did develop granuloma necrosis, albeit to a slightly lesser extent than infected wild-type control mice. That the

overall quantity of bacterial CFU has some role in inducing necrosis, is evident from infection experiments with less virulent strains of *M. avium*, that do not reach the excessive levels of bacterial replication as does TMC724, in which central granuloma necrosis did not occur (16, 27). Our results, however, clearly rule out the existence of a mycobacteria-derived factor directly inducing this organized form of tissue damage.

A novel feature of our experimental system is the use of pulmonary compliance as an independent quantitative parameter for loss of recruitable lung space and/or interstitial elasticity in the course of infection. This parameter has allowed us to objectively compare different groups of KO mice at different stages of infection because their functional respiratory parameters were essentially identical. For instance, although pulmonary compliance was similarly low in wild-type, RAG-1–KO and IL-10–KO mice at 19 wk after infection, histopathology was grossly different; granuloma necrosis was completely absent in RAG-1–KO mice, but accelerated in IL-10–KO mice compared with wild-type mice. IL-12–deficient and αβ TCR-KO mice also exhibited no centrally necrotizing granulomas. However, these mice had a significantly better pulmonary compliance, likely due to the fact that IL-12 and αβ TCR^+ cells are also involved in accelerating inflammation. Therefore, delayed recruitment of inflammatory cells into the lung may be one factor contributing to the lack of granuloma necrosis in αβ TCR- or IL-12–deficient mice. With regard to the differences in pulmonary compliance between RAG-1–KO and αβ TCR-KO mice, it is possible that unbalancing of a subtle cross-regulation of the αβ TCR^+ and the γδ TCR^+ subsets is most evident when only one T cell subset, but not both, is missing.

Our histopathological results with γδ TCR-KO mice are difficult to reconcile with the findings published by Saunders et al. who reported that γδ TCR-KO mice never developed centrally caseating lesions in response to pulmonary *M. avium* infection (27). However, these investigators used a much lower dose of infection (500 CFU/mouse) and examined lung histopathology at relatively early time points (days 90 and 120 after infection). Our own data fit very well with the previously documented antiinflammatory role of γδ TCR-bearing cells in other model systems. For example, γδTCR^+ cells regulate and harness αβ TCR bearing cells in *Listeria monocytogenes* infection, where the absence of γδ TCR^+ cells results in accelerated and enhanced pyogenic necrosis of granulomatous lesions (31, 32). Similarly, *M. tuberculosis* infection in γδTCR-KO mice leads to increased neutrophil influx into granulomas (33).

We found that some CD4-deficient mice had a few small necrotic foci at the centers of granulomatous lesions suggesting that a subset of αβ TCR^+ cells negative for the CD4 marker might be capable of inducing caseation. One subset of αβ TCR^+ cells which is negative for both the CD4 and the CD8 markers has indeed been implicated in the killing of mycobacteria-infected target cells and also of mycobacteria themselves (34). These αβ TCR^+ $CD4^-CD8^-$ cells utilize CD1 as their major restricting element during antigen presentation (35, 36). However, when β2M-KO mice known to be deficient not only in MHC class I, but also in CD1, were infected with *M. avium* by aerosol, they showed no difference in either the kinetics or the extent of granuloma necrosis when compared with wild-type mice. Therefore, it appears reasonable to assume that, as previously demonstrated in CD4-deficient mice infected with *Leishmania major* or *M. tuberculosis* (37, 38), a numerically significant amount of "unusual", compensatory MHC class II–restricted $CD4^-CD8^-$ T cells still exist in these mice that are functional in the same way as $CD4^+$ cells in terms of cytokine secretion and, potentially, membrane-dependent events that may ultimately lead to granuloma necrosis. This hypothesis was corroborated by our experiments in MHC class II-KO mice which had no signs of granuloma necrosis at 19 wk after infection with airborne *M. avium*.

In the search for a mechanism by which αβ TCR-bearing cells would mediate granuloma necrosis we identified IFN-γ as a critical factor. IFN-γ is the major inducer of antibacterial effector functions in mycobacteria-infected macrophages, and also plays a significant role in the formation of organized granulomas in response to mycobacterial infections (39–41). In other model systems, such as autoimmune encephalomyelitis, the absence of IFN-γ causes a highly disorganized, hyperinflammatory response characterized by the increased influx of $CD4^+$ T cells and granulocytes (42, 43). Moreover, infection with mycobacteria was documented previously to cause a severe hematopoietic remodelling in IFN-γ–KO mice, resulting in extramedullary hematopoiesis and marked granulocytosis in the peripheral blood (44). IFN-γ has been shown to induce apoptosis of activated T cells, thereby limiting the inflammatory response, in other experimental systems including that of pulmonary infection with *M. tuberculosis* (43, 45). Although not directly investigated here, the absence of this mechanism may have contributed to the hyperinflammatory response seen here in the absence of IFN-γ.

Our results from infected IL-10– and IL-12–deficient animals are in line with current thinking about the regulation of IFN-γ production. Thus, IL-10 downregulates IFN-γ secretion in vitro and in vivo (46), and the accelerated granuloma necrosis we observed in IL-10–deficient mice may be interpreted as a consequence of increased IFN-γ levels in these mice. Aggravated immunopathology has been observed by other investigators examining autoimmune diseases (47, 48) or intracellular infections (49) in IL-10–KO mice (50), and has generally been attributed to the increased production of IFN-γ in these mice (51).

In a mouse model of intravenous infection with *Cryptococcus neoformans*, the development of granulomas was abolished in IL-12p40-KO mice, but not reduced when IL-12p40 was still present in IL-12p35-KO mice (52). When we infected the same strains of KO mice with *M. avium* by aerosol, we found that pulmonary granuloma necrosis was completely absent, but that there was no difference between mice lacking only p35 or both, p35 and p40 chains

of IL-12 at the time points studied. In contrast to IFN-γ–KO mice, however, inflammation was significantly reduced, rather than exacerbated, as evidenced by increased pulmonary compliance in both IL-12p35-KO and IL-12p35/p40-double-KO mice at week 19.

When interpreting these seemingly paradoxical results in infected IL-12–KO and IFN-γ–KO mice, it should be kept in mind that not all effects of IL-12 are mediated by IFN-γ (53). For instance, when IFN-γR–KO mice were treated with recombinant IL-12, they developed extensive pulmonary macrophage infiltrations and died from diffuse pulmonary edema (54). Conversely, in parallel experiments done in an intravenous model of *M. avium* infection, we observed that IFN-γ is not entirely absent in infected tissues of IL-12–KO mice (unpublished data). Although we did not investigate IFN-γ levels in the lungs of IL-12–KO mice in the studies presented here, we hypothesize that residual, but significantly above-background levels of IFN-γ that are induced even in the absence of IL-12 are sufficient to prevent the highly dysregulated inflammatory response seen in the complete absence of IFN-γ in IFN-γ–KO mice, but are much too low to induce recruitment and activation of inflammatory cells to the level observed in wild-type mice.

One important effector mechanism triggered by IFN-γ is the induction of nitric oxide in macrophages (55). Nitric oxide does not inhibit growth of *M. avium* as it does with *M. tuberculosis* (30, 56), but nitric oxide is involved in the downregulation of the inflammatory response to *M. avium* (57). Nitrogen intermediates and their reaction products can be highly toxic to both tumor and parenchymal cells (55), and we reasoned that granuloma necrosis induced by IFN-γ might be mediated by the tissue-destroying sequelae of NO production in our model. However, results from our experiments with iNOS-KO mice unequivocally show that granuloma necrosis in this model occurs independently of iNOS, although the overall inflammatory dysregulation evident in iNOS-KO mice, with dramatically reduced pulmonary function and premature death of infected mice, was similar to that seen in IFN-γ–KO mice.

These convergent and divergent effects of IFN-γ and iNOS on the overall inflammatory response and the induction of granuloma necrosis may best be explained as follows: IFN-γ modulates a number of quantitative and qualitative aspects of inflammation, such as endothelial molecule expression, vascular leakiness, and leukocyte extravasation, via the induction of nitric oxide (57–59). In addition, during mycobacterial infections, IFN-γ–induced nitric oxide may suppress T cell functions and induce apoptosis of $CD4^+$ T cells thereby controlling excess inflammation (45, 60, 61).

The mechanisms induced by IFN-γ that cause the necrotization of granulomas, however, are clearly distinct from nitric oxide. It is at present unclear whether IFN-γ directly acts on macrophages at the center of the granuloma causing them to necrotize, or whether IFN-γ induces other mediators which in turn cause necrosis. IFN-γ is known to induce several chemokines, and it is intriguing that some of them, such as IFN-γ-inducible protein of 10-kD (IP)-10, monokine induced by IFN-γ (Mig), IFN-inducible T cell α chemoattractant (I-TAC), and secondary lymphoid tissue chemokine (SLC), have profound angiostatic properties (62). It is conceivable that chemokine-mediated reduced vascularization and concomitant hypoxia of granulomas are the ultimate downstream events responsible for caseous necrosis. A similar scenario was recently described for tumor regression during acute *Toxoplasma gondii* infection in mice (63).

Finally, it is worth mentioning that we cannot at present exclude that TNF is also involved in the process of granuloma necrotization. TNF is thought to sensitize infected cells for subsequent necrosis and has been a prime candidate for explaining the Koch phenomenon (22, 64). However, after *M. avium* infection of TNF receptor of 55 kD (TNFRp55)-KO mice by either the aerogenic or the intravenous route, granuloma formation and maintenance are severely impaired very early during infection, and all TNFRp55-KO mice succumb to infection at the same time that granulomas disintegrate (16, 65). Therefore, the role of TNF in granuloma necrosis could not be appropriately addressed in this model.

Dannenberg and Rook used the term "tissue-damaging DTH" for the immune response leading to pathology, i.e., necrotizing lesions, and reserved the term "cell-mediated immunity" for the macrophage-activating immune response leading to bacteriostasis in the course of infection with *M. tuberculosis* (6). The interplay and ratio between these two phenomena remain unknown. Indeed, caseous necrosis and tissue damage may merely be an excess of cell-mediated immunity, or represent an extreme form of protection, as it is clear that mycobacteria do not thrive in caseous lesions (66). It seems a reasonable approach to use the aerosol *M. avium* model system to determine the molecular mediators of tissue damage, and subsequently verify that similar mechanisms are operative in *M. tuberculosis* lesions in human patients. However, extrapolation of our results to protective immunity to TB is not readily possible, because the mechanisms of killing *M. avium* are likely very different from those involved in killing *M. tuberculosis* (28, 30, 56). For this reason, an animal model reflecting human pathology, but using *M. tuberculosis* itself, will be very important. In this regard, it was recently reported that iNOS-KO mice aerogenically infected with *M. tuberculosis* developed lesions similar to those described here (67). One might therefore speculate that very low levels of nitric oxide, such as those presumably present in human lungs, may actually favor the development of caseating necrosis in response to *M. tuberculosis* infection.

From experience with human TB patients, it is well-known that a severe deficiency in the T cell compartment precludes a positive intradermal DTH reaction to tuberculin (68, 69). Moreover, AIDS patients suffering from advanced deficiency in the $CD4^+$ T cell compartment and patients having defects in the IL-12/IFN-γ signaling pathways fail to develop circumscript granulomas and never exhibit extensive caseating necrosis and/or cavitation after *M.*

tuberculosis or *M. avium* infection, but rather develop disseminated disease (70–77). In contrast, AIDS patients with residual disseminated *M. avium* infection develop necrotizing granulomas under antiretroviral therapy as soon as their $CD4^+$ cell number and response is restored (78–80). We take this as evidence that our experimental system in mice is valid in that it reflects at least some processes occurring also in humans infected with mycobacteria. Taking advantage of the ready availability of mouse strains with targeted mutations in candidate molecules, this model can now be employed to define the mediators of granuloma caseation that lie downstream from IFN-γ. This approach may ultimately lead to novel adjuvant therapeutic strategies aimed at inhibiting caseation and liquefaction of the granuloma in order to facilitate antimicrobial chemotherapy and reduce the spread of microorganisms.

We wish to thank Johanna Suwinski, Svenja Kröger-Albrecht, Claudia Hahn, Stefanie Kutsch, and Dörte Karp for expert technical assistance.

This work was supported in part by research grants from the Deutsche Forschungsgemeinschaft (SFB367-C9 to S. Ehlers, SFB367-A9 to S. Uhlig, and AL 371/3-1 to G. Alber).

Submitted: 17 January 2001
Revised: 22 October 2001
Accepted: 8 November 2001

References

1. Dannenberg, A.M., Jr. 1991. Delayed-type hypersensitivity and cell-mediated immunity in the pathogenesis of tuberculosis. *Immunol. Today*. 12:228–233.
2. Cotran, R.S., V. Kumar, and S.L. Robbins. 1994. Inflammation and repair. *In* Robbins Pathologic Basis of Disease. R.S. Cotran, S. Robbins, and V. Kumar, editors. W.B. Saunders Company, Philadelphia, PA. pp. 51–92.
3. Ehlers, S. 1999. Immunity to tuberculosis: a delicate balance between protection and pathology. *FEMS Immunol. Med. Microbiol.* 23:149–158.
4. Dannenberg, A.M., Jr. 1999. Pathophysiology: basic aspects. *In* Tuberculosis and Nontuberculous Mycobacterial Infections. D. Schlossberg, editor. W.B. Saunders Company, Philadelphia, PA. pp. 17–47.
5. Jagirdar, J., and D. Zagzag. 1996. Pathology and insights into pathogenesis of tuberculosis. *In* Tuberculosis. W.N. Rom, and S. Garay, editors. Little, Brown, and Co., Boston, MA. pp. 467–482.
6. Dannenberg, A.M., and G.A.W. Rook. 1994. Pathogenesis of pulmonary tuberculosis: an interplay of tissue-damaging and macrophage-activating immune responses - dual mechanisms that control bacillary multiplication. *In* Tuberculosis: pathogenesis, protection, and control. B.R. Bloom, editor. ASM Press, Washington, DC. pp. 459–483.
7. Patterson, P.E., M.E. Kimerling, W.C. Bailey, and N.E. Dunlap. 1999. Chemotherapy of tuberculosis. *In* Tuberculosis and Nontuberculous Mycobacterial Infections. D. Schlossman, editor. W.B. Saunders Company, Philadelphia, PA. pp. 71–82.
8. Raviglione, M.C., D.E. Snider, Jr., and A. Kochi. 1995. Global epidemiology of tuberculosis. Morbidity and mortality of a worldwide epidemic. *J. Am. Med. Assoc.* 273:220–226.
9. Lopez, A.D., and C.C.J.L. Murray. 1998. The global burden of disease, 1990–2020. *Nat. Med.* 4:1241–1243.
10. Saunders, B.M., and A.M. Cooper. 2000. Restraining mycobacteria: role of granulomas in mycobacterial infections. *Immunol. Cell Biol.* 78:334–341.
11. Rhoades, E.R., A.A. Frank, and I.M. Orme. 1997. Progression of chronic pulmonary tuberculosis in mice aerogenically infected with virulent Mycobacterium tuberculosis. *Tuber. Lung Dis.* 78:57–66.
12. North, R.J. 1995. Mycobacterium tuberculosis is strikingly more virulent for mice when given via the respiratory than via the intravenous route. *J. Infect. Dis.* 172:1550–1553.
13. McMurray, D.N., F.M. Collins, A.M. Dannenberg, Jr., and D.W. Smith. 1996. Pathogenesis of experimental tuberculosis in animal models. *Curr. Top. Microbiol. Immunol.* 215:157–179.
14. Lurie, M.B., S. Abramson, and A.G. Heppleston. 1952. On the response of genetically resistant and susceptible rabbits to the quantitative inhalation of human-type tubercle bacilli and the nature of resistance to tuberculosis. *J. Exp. Med.* 95:119–134.
15. Converse, P.J., A.M. Dannenberg, Jr., J.E. Estep, K. Sugisaki, Y. Abe, B.H. Schofield, and M.L. Pitt. 1996. Cavitary tuberculosis produced in rabbits by aerosolized virulent tubercle bacilli. *Infect. Immun.* 64:4776–4787.
16. Benini, J., E.M. Ehlers, and S. Ehlers. 1999. Different types of pulmonary granuloma necrosis in immunocompetent vs. TNFRp55-gene-deficient mice aerogenically infected with highly virulent Mycobacterium avium. *J. Pathol.* 189:127–137.
17. Cooper, A.M., and J.L. Flynn. 1995. The protective immune response to Mycobacterium tuberculosis. *Curr. Opin. Immunol.* 7:512–516.
18. Held, H.D., and S. Uhlig. 2000. Basal lung mechanics and airway and pulmonary vascular responsiveness in different inbred mouse strains. *J. Appl. Physiol.* 88:2192–2198.
19. von Bethmann, A.N., F. Brasch, R. Nusing, K. Vogt, H.D. Volk, K.M. Muller, A. Wendel, and S. Uhlig. 1998. Hyperventilation induces release of cytokines from perfused mouse lung. *Am. J. Respir. Crit. Care Med.* 157:263–272.
20. Koch, R. 1891. Fortsetzung über ein Heilmittel gegen Tuberkulose. *Dtsch. Med. Wochenschr.* 17:101–102.
21. Anderson, M.C. 1891. On Koch's treatment. *Lancet.* 1:651–652.
22. Rook, G.A., and J.L. Stanford. 1996. The Koch phenomenon and the immunopathology of tuberculosis. *Curr. Top. Microbiol. Immunol.* 215:239–262.
23. Rook, G.A.W., and B.R. Bloom. 1994. Mechanisms of pathogenesis in tuberculosis. *In* Tuberculosis: protection, pathology and control. B.R. Bloom, editor. 1994. ASM Press, Washington, D.C. pp. 485–502.
24. Inderlied, C.B., C.A. Kemper, and L.E. Bermudez. 1993. The Mycobacterium avium complex. *Clin. Microbiol. Rev.* 6:266–310.
25. Iseman, M.D. 1989. Mycobacterium avium complex and the normal host: the other side of the coin. *N. Engl. J. Med.* 321: 896–898.
26. Dunn, P.L., and R.J. North. 1995. Virulence ranking of some Mycobacterium tuberculosis and Mycobacterium bovis strains according to their ability to multiply in the lungs, induce lung pathology, and cause mortality in mice. *Infect. Immun.* 63:3428–3437.
27. Saunders, B.M., A.A. Frank, A.M. Cooper, and I.M. Orme.

1998. Role of γδ T cells in immunopathology of pulmonary Mycobacterium avium infection in mice. *Infect. Immun.* 66: 5508–5514.
28. Mogues,T., M.E. Goodrich, L. Ryan, R. LaCourse, and R.J. North. 2001. The relative importance of T cell subsets in immunity and immunopathology of airborne *Mycobacterium tuberculosis* infection in mice. *J. Exp. Med.* 193:271–280.
29. Flynn, J.L., and J. Chan. 2001. Immunology of tuberculosis. *Annu. Rev. Immunol.* 19:93–129.
30. Gomes, M.S., M. Florido, T.F. Pais, and R. Appelberg. 1999. Improved clearance of Mycobacterium avium upon disruption of the inducible nitric oxide synthase gene. *J. Immunol.* 162:6734–6739.
31. Thoma-Uszynski, S., C.H. Ladel, and S.H. Kaufmann. 1997. Abscess formation in Listeria monocytogenes-infected γδ T cell deficient mouse mutants involves αβ T cells. *Microb. Pathog.* 22:123–128.
32. Mombaerts, P., J. Arnoldi, F. Russ, S. Tonegawa, and S.H. Kaufmann. 1993. Different roles of αβ and γδ T cells in immunity against an intracellular bacterial pathogen. *Nature.* 365:53–56.
33. D'Souza, C.D., A.M. Cooper, A.A. Frank, R.J. Mazzaccaro, B.R. Bloom, and I.M. Orme. 1997. An anti-inflammatory role for γδ T lymphocytes in acquired immunity to Mycobacterium tuberculosis. *J. Immunol.* 158:1217–1221.
34. Stenger, S., R.J. Mazzaccaro, K. Uyemura, S. Cho, P.F. Barnes, J.P. Rosat, A. Sette, M.B. Brenner, S.A. Porcelli, B.R. Bloom, and R.L. Modlin. 1997. Differential effects of cytolytic T cell subsets on intracellular infection. *Science.* 276: 1684–1687.
35. Beckman, E.M., S.A. Porcelli, C.T. Morita, S.M. Behar, S.T. Furlong, and M.B. Brenner. 1994. Recognition of a lipid antigen by CD1-restricted $\alpha\beta^+$ T cells. *Nature.* 372:691–694.
36. Porcelli, S.A., and R.L. Modlin. 1999. The CD^+ system: antigen-presenting molecules for T cell recognition of lipids and glycolipids. *Annu. Rev. Immunol.* 17:297–329.
37. Locksley, R.M., S.L. Reiner, F. Hatam, D.R. Littman, and N. Killeen. 1993. Helper T cells without CD4: control of leishmaniasis in CD4-deficient mice. *Science.* 261:1448–1451.
38. Caruso, A.M., N. Serbina, E. Klein, K. Triebold, B.R. Bloom, and J.L. Flynn. 1999. Mice deficient in CD4 T cells have only transiently diminished levels of IFN-γ, yet succumb to tuberculosis. *J. Immunol.* 162:5407–5416.
39. Cooper, A.M., D.K. Dalton, T.A. Stewart, J.P. Griffin, D.G. Russell, and I.M. Orme. 1993. Disseminated tuberculosis in interferon γ gene-disrupted mice. *J. Exp. Med.* 178:2243–2247.
40. Flynn, J.L., J. Chan, K.J. Triebold, D.K. Dalton, T.A. Stewart, and B.R. Bloom. 1993. An essential role for interferon γ in resistance to Mycobacterium tuberculosis infection. *J. Exp. Med.* 178:2249–2254.
41. Smith, D., H. Hansch, G. Bancroft, and S. Ehlers. 1997. T-cell-independent granuloma formation in response to Mycobacterium avium: role of tumour necrosis factor-α and interferon-γ. *Immunology.* 92:413–421.
42. Ferber, I.A., S. Brocke, C. Taylor-Edwards, W. Ridgway, C. Dinisco, L. Steinman, D. Dalton, and C.G. Fathman. 1996. Mice with a disrupted IFN-γ gene are susceptible to the induction of experimental autoimmune encephalomyelitis (EAE). *J. Immunol.* 156:5–7.
43. Chu, C.Q., S. Wittmer, and D.K. Dalton. 2000. Failure to suppress the expansion of the activated CD4 T cell population in interferon γ-deficient mice leads to exacerbation of experimental autoimmune encephalomyelitis. *J. Exp. Med.* 192:123–128.
44. Murray, P.J., R.A. Young, and G.Q. Daley. 1998. Hematopoietic remodeling in interferon-γ-deficient mice infected with mycobacteria. *Blood.* 91:2914–2924.
45. Dalton, D.K., L. Haynes, C.Q. Chu, S.L. Swain, and S. Wittmer. 2000. Interferon γ eliminates responding CD4 T cells during mycobacterial infection by inducing apoptosis of activated CD4 T cells. *J. Exp. Med.* 192:117–122.
46. Moore, K.W., M.R. de Waal, R.L. Coffman, and A. O'Garra. 2001. Interleukin-10 and the interleukin-10 receptor. *Annu. Rev. Immunol.* 19:683–765.
47. Bettelli, E., M.P. Das, E.D. Howard, H.L. Weiner, R.A. Sobel, and V.K. Kuchroo. 1998. IL-10 is critical in the regulation of autoimmune encephalomyelitis as demonstrated by studies of IL-10- and IL-4-deficient and transgenic mice. *J. Immunol.* 161:3299–3306.
48. Asseman, C., S. Mauze, M.W. Leach, R.L. Coffman, and F. Powrie. 1999. An essential role for interleukin 10 in the function of regulatory T cells that inhibit intestinal inflammation. *J. Exp. Med.* 190:995–1004.
49. Gazzinelli, R.T., M. Wysocka, S. Hieny, T. Scharton-Kersten, A. Cheever, R. Kuhn, W. Muller, G. Trinchieri, and A. Sher. 1996. In the absence of endogenous IL-10, mice acutely infected with Toxoplasma gondii succumb to a lethal immune response dependent on $CD4^+$ T cells and accompanied by overproduction of IL-12, IFN-γ and TNF-α. *J. Immunol.* 157:798–805.
50. Holscher, C., M. Mohrs, W.J. Dai, G. Kohler, B. Ryffel, G.A. Schaub, H. Mossmann, and F. Brombacher. 2000. Tumor necrosis factor α-mediated toxic shock in Trypanosoma cruzi-infected interleukin 10-deficient mice. *Infect. Immun.* 68:4075–4083.
51. de Vries, J.E. 1995. Immunosuppressive and anti-inflammatory properties of interleukin 10. *Ann. Med.* 27:537–541.
52. Decken, K., G. Kohler, K. Palmer-Lehmann, A. Wunderlin, F. Mattner, J. Magram, M.K. Gately, and G. Alber. 1998. Interleukin-12 is essential for a protective Th1 response in mice infected with Cryptococcus neoformans. *Infect. Immun.* 66: 4994–5000.
53. Gately, M.K., L.M. Renzetti, J. Magram, A.S. Stern, L. Adorini, U. Gubler, and D.H. Presky. 1998. The interleukin-12/interleukin-12-receptor system: role in normal and pathologic immune responses. *Annu. Rev. Immunol.* 16:495–521.
54. Car, B.D., V.M. Eng, B. Schnyder, M. LeHir, A.N. Shakhov, G. Woerly, S. Huang, M. Aguet, T.D. Anderson, and B. Ryffel. 1995. Role of interferon-γ in interleukin 12-induced pathology in mice. *Am. J. Pathol.* 147:1693–1707.
55. MacMicking, J., Q.W. Xie, and C. Nathan. 1997. Nitric oxide and macrophage function. *Annu. Rev. Immunol.* 15:323–350.
56. MacMicking, J.D., R.J. North, R. LaCourse, J.S. Mudgett, S.K. Shah, and C.F. Nathan. 1997. Identification of nitric oxide synthase as a protective locus against tuberculosis. *Proc. Natl. Acad. Sci. USA.* 94:5243–5248.
57. Ehlers, S., S. Kutsch, J. Benini, A. Cooper, C. Hahn, J. Gerdes, I. Orme, C. Martin, and E.T. Rietschel. 1999. NOS2-derived nitric oxide regulates the size, quantity and quality of granuloma formation in Mycobacterium avium-infected mice without affecting bacterial loads. *Immunology.* 98:313–323.
58. Spiecker, M., H. Darius, K. Kaboth, F. Hubner, and J.K.

Liao. 1998. Differential regulation of endothelial cell adhesion molecule expression by nitric oxide donors and antioxidants. *J. Leukoc. Biol.* 63:732–739.
59. Lyons, C.R. 1995. The role of nitric oxide in inflammation. *Adv. Immunol.* 60:323-371.
60. Tomioka, H., K. Sato, W.W. Maw, and H. Saito. 1995. The role of tumor necrosis factor, interferon-γ, transforming growth factor-β, and nitric oxide in the expression of immunosuppressive functions of splenic macrophages induced by Mycobacterium avium complex infection. *J. Leukoc. Biol.* 58: 704–712.
61. Nabeshima, S., M. Nomoto, G. Matsuzaki, K. Kishihara, H. Taniguchi, S. Yoshida, and K. Nomoto. 1999. T-cell hyporesponsiveness induced by activated macrophages through nitric oxide production in mice infected with Mycobacterium tuberculosis. *Infect. Immun.* 67:3221–3226.
62. Oppenheim, J.J., O.M. Zack Howard, and E. Goetzl. 2001. Chemotactic factors, neuropeptides, and other ligands for seven transmembrane receptors. *In* Cytokine Reference, Volume I. J.J. Oppenheim and M. Feldmann, editors. Academic Press, San Diego, CA. pp. 985–1021.
63. Hunter, C.A., D. Yu, M. Gee, C.V. Ngo, C. Sevignani, M. Goldschmidt, T.V. Golovkina, S. Evans, W.F. Lee, and A. Thomas-Tikhonenko. 2001. Cutting edge: systemic inhibition of angiogenesis underlies resistance to tumors during acute toxoplasmosis. *J. Immunol.* 166:5878–5881.
64. Rook, G.A., and R. Attiyah. 1991. Cytokines and the Koch phenomenon. *Tubercle*. 72:13–20.
65. Ehlers, S., S. Kutsch, E.M. Ehlers, J. Benini, and K. Pfeffer. 2000. Lethal granuloma disintegration in mycobacteria-infected TNFRp55$^{-/-}$ mice is dependent on T cells and IL-12. *J. Immunol.* 165:483–492.
66. Moulding, T. 1999. Pathogenesis, pathophysiology, and immunology: clinical orientations. *In* Tuberculosis and Nontuberculous Mycobacterial Infections. D. Schlossberg, editor. W.B. Saunders Company, Philadelphia, PA. pp. 48–56.
67. Cooper, A.M., J.E. Pearl, J.V. Brooks, S. Ehlers, and I.M. Orme. 2000. Expression of the nitric oxide synthase 2 gene is not essential for early control of Mycobacterium tuberculosis in the murine lung. *Infect. Immun.* 68:6879–6882.
68. Lordi, G.M., and L.B. Reichman. 1999. Tuberculin skin testing. *In* Tuberculosis and Nontuberculous Mycobacterial Infections. D. Schlossberg, editor. W.B. Saunders Company, Philadelphia, PA. pp. 65–70.
69. Garay, S.M. 2000. Tuberculosis and the human immunodeficiency virus infection. *In* Tuberculosis. W.N. Rom, and S. Garay, editors. Little, Brown, and Company, Boston, MA. pp. 443–465.
70. Di Perri, G., A. Cazzadori, S. Vento, S. Bonora, M. Malena, L. Bontempini, M. Lanzafame, B. Allegranzi, and E. Concia. 1996. Comparative histopathological study of pulmonary tuberculosis in human immunodeficiency virus-infected and non-infected patients. *Tuber. Lung Dis.* 77:244–249.
71. Dorman, S.E., and S.M. Holland. 1998. Mutation in the signal-transducing chain of the interferon-γ receptor and susceptibility to mycobacterial infection. *J. Clin. Invest.* 101: 2364–2369.
72. Altare, F., A. Durandy, D. Lammas, J.F. Emile, S. Lamhamedi, F. Le Deist, P. Drysdale, E. Jouanguy, R. Doffinger, F. Bernaudin, O. Jeppsson, J.A. Gollob, et al. 1998. Impairment of mycobacterial immunity in human interleukin-12 receptor deficiency. *Science.* 280:1432–1435.
73. Muller, H., and S. Kruger. 1994. Immunohistochemical analysis of cell composition and in situ cytokine expression in HIV- and non-HIV-associated tuberculous lymphadenitis. *Immunobiology*. 191:354–368.
74. Hill, A.R., S. Premkumar, S. Brustein, K. Vaidya, S. Powell, P.W. Li, and B. Suster. 1991. Disseminated tuberculosis in the acquired immunodeficiency syndrome era. *Am. Rev. Respir. Dis.* 144:1164–1170.
75. Small, P.M., and U.M. Selcer. 2000. Human immunodeficiency virus and tuberculosis. *In* Tuberculosis and Nontuberculous Mycobacterial Infections. D. Schlossberg, editor. W.B. Saunders Company, Philadelphia, PA. pp. 329–338.
76. Goodman, P.C. 1990. Pulmonary tuberculosis in patients with acquired immunodeficiency syndrome. *J. Thorac. Imaging.* 5:38–45.
77. Jagadha, V., R.H. Andavolu, and C.T. Huang. 1985. Granulomatous inflammation in the acquired immune deficiency syndrome. *Am. J. Clin. Pathol.* 84:598–602.
78. Foudraine, N.A., E. Hovenkamp, D.W. Notermans, P.L. Meenhorst, M.R. Klein, J.M. Lange, F. Miedema, and P. Reiss. 1999. Immunopathology as a result of highly active antiretroviral therapy in HIV-1-infected patients. *AIDS.* 13: 177–184.
79. Phillips, P., M.B. Kwiatkowski, M. Copland, K. Craib, and J. Montaner. 1999. Mycobacterial lymphadenitis associated with the initiation of combination antiretroviral therapy. *J. Acquirs. Immune. Defic. Syndr. Hum. Retrovirol.* 20:122–128.
80. Race, E.M., J. Adelson-Mitty, G.R. Kriegel, T.F. Barlam, K.A. Reimann, N.L. Letvin, and A.J. Japour. 1998. Focal mycobacterial lymphadenitis following initiation of protease-inhibitor therapy in patients with advanced HIV-1 disease. *Lancet.* 351:252–255.